ACTA ACUSTICA UNITED WITH ACUSTICA
Vol. 103 (2017) 903 – 916

DOI 10.3813/AAA.919119

Which Methods and Strategies to Cope with Noise Complexity for an Effective Interpretation of Acoustic Emission Signals in Noisy Nuclear Environment?

O. I. Traore[1)], N. Favretto-Cristini[1)], L. Pantera[2)], P. Cristini[1)], S. Viguier-Pla[3,4)], P. Vieu[3)]
[1)] Aix-Marseille Univ., CNRS, Centrale Marseille, LMA, France. favretto@lma.cnrs-mrs.fr
[2)] CEA, DEN, DER/SRES, Cadarache, 13108 Saint-Paul-Lez-Durance, France
[3)] Equipe de Stat. et Proba., Institut de Mathématiques, UMR5219, Université Paul Sabatier, 118 Route de Narbonne, 31062 Toulouse Cedex 9, France
[4)] Université de Perpignan via Domitia, LAMPS, 52 av. Paul Alduy, 66860 Perpignan Cedex 9, France

Summary
Prior to an effective interpretation of AE signals in noisy nuclear environment, it is necessary to define an appropriate strategy for detecting structural changes and denoising signals, according to the stochastic behavior of the noise and its level. The ability and efficiency of various methods are studied here. One conclusion of this work is that there is no absolute method which is efficient regardless the type of noise and its level. In a high SNR context, the continuous wavelet transform method is the best tool for analysis of the signal structure, whatever the type of noise. On the contrary, in low SNR context, the detectability of the AE events strongly depends on the type of noise. For denoising problem, the spectral subtraction and the singular spectrum analysis methods are robust to changes in the stochastic behavior of noise. However, the spectral subtraction has a higher SNR improvement potential. We suggest that each selected method can be combined with the other ones in order to further improve the denoising efficiency and to get excellent results regardless the type of noise. The impact of the different selected denoising methods on some classical AE parameters shows that, whatever the type of noise and the denoising method, AE parameters associated with the waveform are better restored than those associated with the acoustic activity and the frequency content.

PACS no. 43.60.-c

Introduction

Several non-destructive methods are used in nuclear industry to inspect the reactors and to get information on the behavior of some of their specific components. Among them, the acoustic emission (AE) technique is a powerful tool which has the advantage of being simple to adapt to nuclear-oriented purposes. In nuclear industry, it has thus been used mainly to monitor the pressure vessels and the primary circuit [1, 2, 3, 4, 5]. More recently, it has been used to monitor the compaction of nuclear fuel powders [6, 7] as well. Whatever the non-destructive testing method, one of the trickiest tasks is the effective interpretation and exploitation of the received information. This is even more important for AE testing. The received information is composed of numerous transient signals resulting from wave propagation generated by unknown source mechanisms of interest, and potentially corrupted by several parameters among which the choice and the settings of the AE acquisition system [8, 9], the environmental noise and the wave propagation path in the structure. From a mathematical point of view, if the environmental noise n is assumed to be additive, the received AE signal x can be written as

$$x(t) = h_1 * h_2 * s(t) + n(t), \quad t \in \{1, \ldots, N\}, \quad (1)$$

where h_1 and h_2 correspond to the impact of the structure and the acquisition system, respectively, s being the signal associated with the physical source mechanism of interest and t the time. One of the key problems of a AE testing process being the estimation of the source signal s, the functions h_1, h_2 and n have to be studied in order to be properly removed from the recorded signal x. In general, h_2 is obtained from the calibration tests of the acquisition system and deconvolution is then sufficient to remove its potential impact on x [10]. On the contrary, evaluating h_1 is quite tricky, and in complex environments numerical simulations of wave propagation can be of help. Since ways of evaluation of h_1 and h_2 are beyond the scope of

Received 3 April 2017,
accepted 30 September 2017.

Author's complimentary copy

the paper of interest here, we will assume hereafter that these functions are known. Therefore, in this case, being able to evaluate and cope with the environmental noise n is the last crucial step for an effective interpretation and exploitation of the received information, and Eq. (1) can be simplified as

$$x(t) = s(t) + n(t), \quad t \in \{1, \ldots, N\}. \tag{2}$$

The environment of industrial reactors is very noisy and the potential sources of n are numerous. Furthermore, in the case of research reactors the experimental protocol must be taken into account as well. Therefore, it is usual to observe fluctuations in the noise level and/or its stochastic behavior, which has an impact on the recorded signals. Indeed, depending on its type, noise can introduce, for instance, undulations which modify the signal envelope and distort some AE parameters. When the noise level is constant and remains below a given threshold, classical thresholding is sufficient to identify the segments of x which are associated with AE events, and then with potential physical source mechanisms of interest. However, if the noise level varies and exceeds the chosen threshold, acoustic events associated with low energetic source mechanisms cannot be detected. More sophisticated methods for structural change detection are therefore necessary to denoise acoustic signals. As a matter of fact, denoising the received signal prior to identifying the associated source mechanism is highly recommended, even in high signal-to-noise ratio (SNR) context.

Detection of structural changes and signal denoising are widely studied in signal processing literature. The different methods used can be classified following several philosophies [11, 12, 13, 14]. For instance, Barat *et al.* [12] suggest a classification of AE filtering methods according to the type of noise and the complexity of the method implementation. Different approaches, from traditional frequency filtering to principal component methods of noise filtering, are thus presented. For our purpose, we shall adopt here the same philosophy and consider some time domain, frequency domain and time-frequency decomposition-based methods of interest. Our work goes beyond the straightforward application of these methods to our topic. We compare their potential for SNR improvement. In addition, we want to improve the global performance of each method, possibly not adapted to process a given type of noise, by wisely combining this method with other ones. The interest lies in the fact that, taken alone or applied jointly with some others, a chosen method could cope with all the potential problems of detection of structural changes and signal denoising in nuclear context. Therefore, the goal of our work is twofold. We want to define efficient strategies for detecting the structural changes and denoising AE signals, whatever the type and level of noise encountered in nuclear safety experiments. In addition, we want to evaluate the impact of denoising methods on typical and widely used AE parameters. We keep in mind that some of them might be crucial for an efficient subsequent identification of the physical source mechanisms associated with the recorded acoustic events. Therefore, they must be preserved as much as possible.

The paper is then organized as follows. In Section 1, we present the nuclear safety experimentations, and more specifically the typical signals recorded and the main types of noise observed during experiments. Section 2 briefly reviews the methods of interest (namely, the spectral subtraction and the short Fourier transform, the singular spectrum analysis, and the wavelet transforms). For each one, we mention the application domain and the level of the implementation complexity. Detection of the structural changes of the signals, according to the type and level of noise, is studied in Section 3. Section 4 is devoted to the signal denoising. We compare the efficiency of the selected methods for SNR improvement. Their impact on the AE parameters is also investigated. Finally, results obtained permit us to suggest efficient strategies for handling noisy AE signals whatever the context.

1. Experimental data and potential types of noise in nuclear environments

The experimental data of interest here have been collected during different Reactivity Initiated Accidents (RIA) experiments performed at the French Atomic Energy Commission (CEA) research center of Cadarache in southern France. RIA is a nuclear reactor accident which may damage the reactor core, and in severe cases, even lead to disruption of the reactor. It involves an unwanted increase in fission rate and reactor power. This power excursion may lead to failure of the fuel rods and release of radioactive material into the primary reactor coolant. This material comprises gaseous fission products as well as fuel pellet solid fragments. In severe cases, the fuel rods may be shattered, and large parts of the fuel pellet inventory dispersed into the coolant. The expulsion of hot fuel into water has potential to cause rapid steam generation and pressure pulses, which could damage nearby fuel assemblies, other core components, and possibly also the reactor vessel [15].

The RIA experiments are performed in an open pool-type research reactor composed of a driver core made of a thousand of UO_2 rods and specially designed to support an injection of reactivity. The reactor includes an experimental loop specially designed to receive, in the center of the driver core, the instrumented test device housing the fuel rod to be tested. This test device corresponds to a stratified medium with different types of fine layers of few millimeters, from the fuel rod of UO_2 to the external layer of Zircaloy (cf. Figures 1 and 2). The test device is equipped with several sensors (including two piezoelectric AE sensors) to control the experiment and to characterize the behavior of the fuel rod during the power burst. The AE sensors are made of lithium niobate cristal with a passband of 5–400 kHz and designed to work in nuclear harsh environment up to 600 degrees Celsius. They are located at the top and the bottom of the fuel rod, respectively, and

Author's complimentary copy

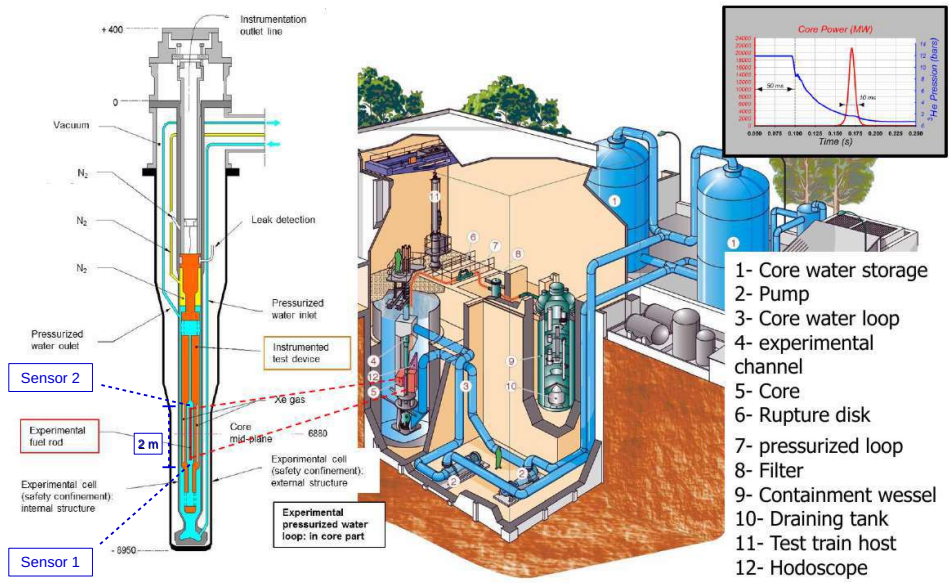

Figure 1. Sketch of the RIA experimental reactor and the test device containing the fuel sample.

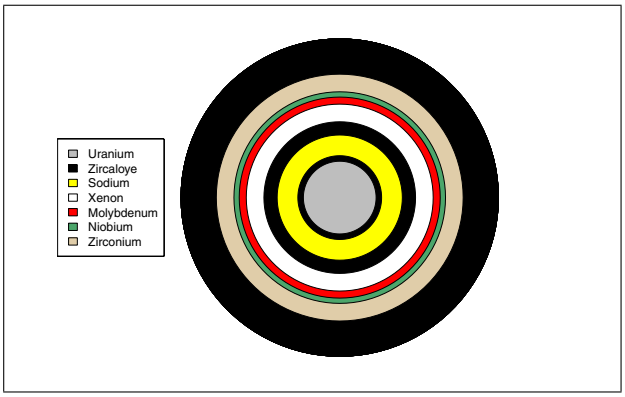

Figure 2. Radial section of the test device at $z = 0$ illustrating the different types of media involved. Note that the number and the type of the layers can change depending on the position on the $z - axis$ and that the scale of the illustration is not real although representative.

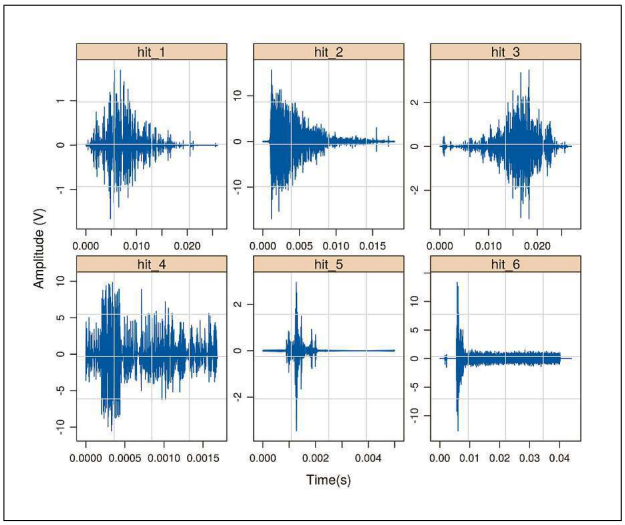

Figure 3. Acoustic events selected for illustration purposes. Some classical AE parameters associated with them are depicted in Table I.

are distant of 2 m (Figure 1). A (40 dB) preamplifier is associated with each sensor. The sampling rate is 2.5 µs.

Among the acoustic events detected by the two sensors during RIA experiments, some are generated by the above-mentioned direct consequences of these severe problems (e.g., failures of the fuel rods, fuel ejections, gas leakages and fuel/clad interaction); others are suspected to be generated by source mechanisms not yet well identified. Since one of the challenging goal, when using AE technique, is to detect all the events in an efficient way, no strong assumption on the nature of the physical source mechanisms is made hereafter.

After each experiment, a post-processing of the recorded signals is performed to detect the events of interest from the whole experimental signal [16]. Since 1993, fourteen RIA experiments have been performed and 168 acoustic events have been detected. For illustration purposes of our work, we have selected only six events which are supposed to be free from the impacts of h_1, h_2 and n and to correspond exactly to the source s. According to their waveforms (Figure 3) and spectra (Figure 4), these six events are probably associated with six different types of source mechanisms. They have been concatenated in order to form an illustrative source signal s (Figure 6). In addition, three main types of noise have been observed during the fourteen nuclear safety experiments : a classical gaussian white noise characterized by its very wide-band spectrum (Figure 5a), an electric noise (Figure 5b), and a mixed noise (Figure 5c) mainly composed of a very low-frequency component (characterized by undulation) and a very high-frequency component corresponding to the resonance of the test device. We also consider a fourth type

Author's complimentary copy

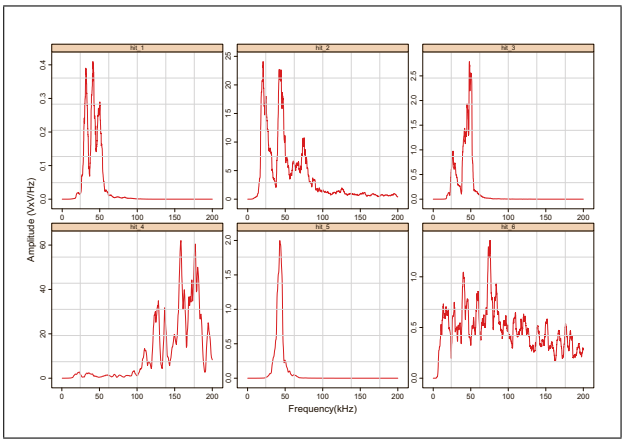

Figure 4. Spectra associated with the six events presented in Figure 3.

of noise artificially created by summing the three previous ones (Figure 5d). This noise corresponds to a very complex one which is rarely encountered in practice, but is of interest for illustration purposes of our work.

2. Review of some methods for detecting structural changes and denoising

Since noise level and noise behavior are of various types (random, deterministic, stationary,...) in industrial reactor environment, we briefly review different methods, with specific assumptions on the noise properties, which are relevant to detect structural changes and denoise signals. Besides a brief recall on their specific mathematical formulation which helps understanding the results presented in the subsequent section, we focus on the practical key points which have to be taken into account when using each method.

2.1. Short-time Fourier transform and Spectral subtraction

2.1.1. Short-Time Fourier Transform

The short-time Fourier transform is a time-frequency method allowing to analyze the structure of a signal, and then to detect the structural changes. It consists in dividing the received signal x into several blocks (also called segments) of equal length, and then computing the Fourier transform separately for each shorter segment,

$$\mathrm{STFT}(n,m) = \sum_{k=0}^{N-1} x(k)\, w(n-k)\, \mathrm{e}^{-\mathrm{j}2\pi km/N},$$

where $w(\beta)$ is the window function of length β (usually a hanning window).

The window length determines the time-frequency resolution of the STFT. Decreasing (respectively, increasing) this length implies a decrease (respectively, increase) in the frequency resolution and an increase (respectively, decrease) in the time resolution [11].

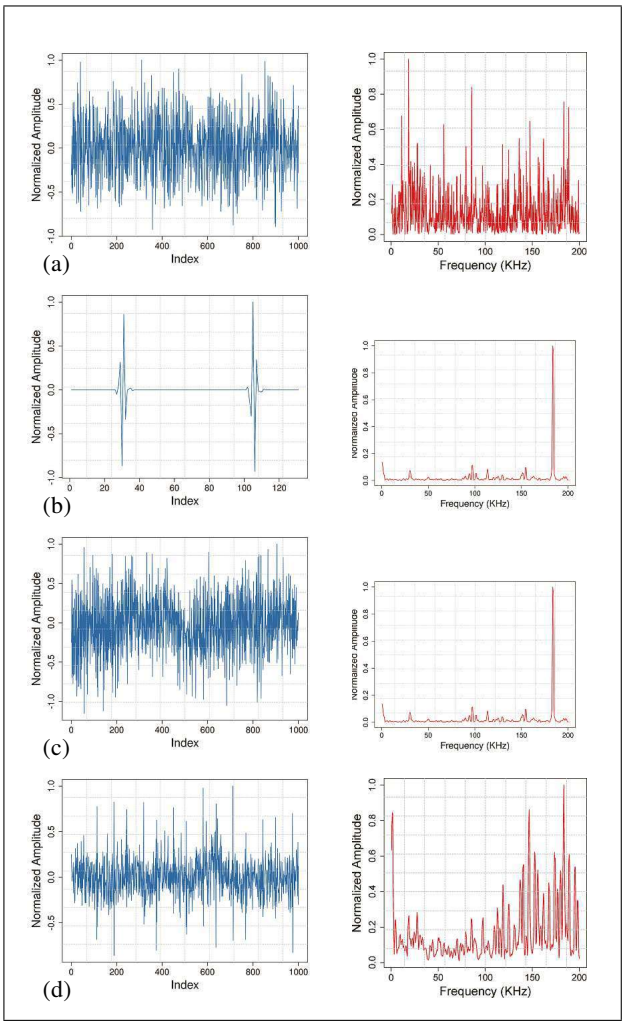

Figure 5. Selected types of noise and associated spectra. (a) simulated gaussian white noise, (b) electric noise, (c) mixed noise recorded during a nuclear safety experiment, and (d) sum of all types of noise.

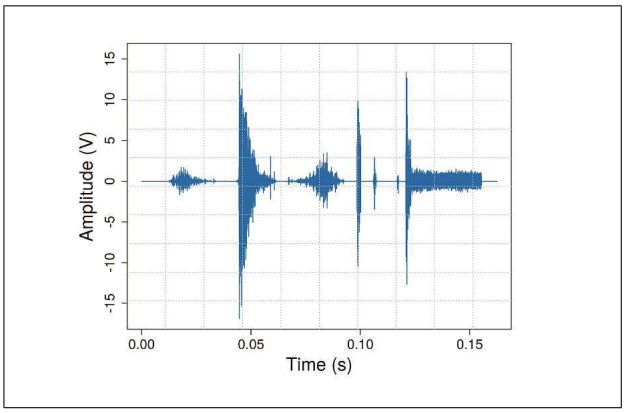

Figure 6. Source signal s corresponding to the concatenation of the six events presented in Figure 3.

2.1.2. Spectral Subtraction (SS)

Introduced by Boll in 1979 [17] and widely used for speech enhancement works [18, 19], the SS has proved good ability in denoising AE signals in some recent works

Author's complimentary copy

Table I. Some classical AE parameters of the six hits computed from the noise-free signal.

	hit_1	hit_2	hit_3	hit_4	hit_5	hit_6
Envelopes correlation	1.00	1.00	1.00	1.00	1.00	1.00
Kullback-Leiber distance	0.00	0.00	0.00	0.00	0.00	0.00
Absolute energy (MV)	12.05	1458.37	59.30	4224.40	31.68	81.15
Amplitude (V)	4.55	23.88	10.82	19.89	9.39	19.43
Count	1135.00	842.00	1186.00	250.00	204.00	3841.00
Mean frequency (kHz)	43.65	46.75	43.90	147.93	40.80	87.29
Rise Time (ms)	6.84	1.20	18.31	0.34	1.27	5.82
Count to pic	306.00	51.00	797.00	58.00	51.00	129.00

Table II. Some classical AE parameters of the six hits computed from the signal denoised by SS in the case of a gaussian white noise.

	hit_1	hit_2	hit_3	hit_4	hit_5	hit_6
Envelopes correlation	0.59	0.99	0.96	0.85	0.94	0.97
Kullback-Leiber distance	8.46	0.44	2.26	1.17	1.69	0.88
Absolute energy (MV)	4.25	696.55	15.37	1439.10	19.29	51.80
Amplitude (V)	-7.39	21.35	3.58	18.79	5.93	18.68
Count	3317.00	1843.00	3136.00	250.00	608.00	5687.00
Mean frequency (kHz)	127.58	102.33	116.07	147.93	121.60	129.24
Rise Time (ms)	8.24	1.25	18.31	0.32	1.27	5.82
Count to pic	1071.00	148.00	2064.00	53.00	157.00	788.00

Table III. Some classical AE parameters of the six hits computed from the signal denoised by wavelet shrinkage in the case of a gaussian white noise.

	hit_1	hit_2	hit_3	hit_4	hit_5	hit_6
Envelopes correlation	0.83	0.99	0.89	0.99	0.87	0.94
Kullback-Leiber distance	1.43	0.15	1.01	0.14	0.46	0.53
Absolute energy (MV)	0.03	585.47	2.40	1787.42	5.24	44.15
Amplitude (V)	-10.95	22.77	3.46	17.23	4.69	19.66
Count	128.00	475.00	384.00	235.00	34.00	333.00
Mean frequency (kHz)	4.92	26.37	14.21	139.05	6.80	7.57
Rise Time (ms)	5.64	1.20	16.62	0.34	1.27	6.04
Count to pic	44.00	14.00	190.00	54.00	5.00	56.00

[20, 21]. It is based on a fundamental assumption: noise is a stationary or slowly varying process, and an estimator $\hat{n}$ of noise n is available.

If we denote by X, S, and N the Fourier transforms of x, s, and n respectively, the SS estimates the spectrum S of the source signal through

$$\hat{S}(f) = \left[\left|X(f)\right| - \alpha\left|\hat{N}(f)\right|\right] \mathrm{e}^{\mathrm{i}\theta_x(f)}, \tag{3}$$

where $\theta_x(f)$ is the phase of the received signal at the frequency f, and α is an over-subtraction parameter allowing to amplify the noise energy. The main difficulty in applying the SS lies in the existence of waveform distortions introduced by the estimation errors due to the random variations of noise. One of the major sources for these distortions is the negative or small-valued spectral estimates of the source signal (see [22], chap.9). Among several approaches proposed by Boll, the half-wave rectification is widely used in order to cope with such a limitation of the SS. It consists in replacing $\hat{S}(f)$ by zero when $\alpha|\hat{N}(f)| > |X(f)|$.

From a practical point of view, implementation of the SS first consists in dividing the received signal into a certain number of overlapping blocks. The SS is then applied on each block in order to estimate the spectrum of the associated source signal, which is transformed back to the time domain by an inverse Fourier transform. Each signal block is then overlapped and added to the preceeding and succeeding blocks to form the final output. Note that the choice of the block length for spectral analysis is a trade-off between conflicting requirements to both the time resolution and the spectral resolution. Therefore, a special attention has to be paid to it (see [22] chap.9, and [21]).

2.2. Singular Spectrum Analysis (SSA)

The main purpose of SSA is to decompose the received signal x into a sum of a small number of independent signals representing components of interest and noise. The SSA technique consists of two complementary stages: decomposition and reconstruction, each of them including two separate steps. Here we summarize the different stages

Author's complimentary copy

Table IV. Some classical AE parameters of the six hits computed from the signal denoised by the SSA in the case of a gaussian white noise.

	hit_1	hit_2	hit_3	hit_4	hit_5	hit_6
Envelopes correlation	0.93	1.00	0.94	0.71	0.96	0.98
Kullback-Leiber distance	2.42	1.30	0.78	3.05	2.36	4.23
Absolute energy (MV)	19.73	1103.87	73.60	873.82	59.61	91.26
Amplitude (V)	2.75	20.88	10.01	14.16	7.46	17.76
Count	2775.00	1443.00	2585.00	259.00	543.00	4740.00
Mean frequency (kHz)	106.73	80.12	95.68	153.25	108.60	107.72
Rise Time (ms)	5.64	2.21	18.31	0.40	1.29	6.04
Count to pic	605.00	182.00	1774.00	61.00	144.00	678.00

Table V. Some classical AE parameters of the six hits computed from the signal denoised by SS in the case of an electric noise.

	hit_1	hit_2	hit_3	hit_4	hit_5	hit_6
Envelopes correlation	1.00	1.00	1.00	0.72	1.00	0.99
Kullback-Leiber distance	0.17	0.27	0.11	1.05	0.06	0.76
Absolute energy (MV)	9.52	1210.93	51.50	1021.68	26.15	89.67
Amplitude (V)	2.36	23.34	10.53	15.92	8.42	21.65
Count	2098.00	885.00	1599.00	242.00	505.00	5004.00
Mean frequency (kHz)	80.69	49.14	59.18	143.20	101.00	113.72
Rise Time (ms)	5.64	1.20	16.62	0.72	1.27	5.82
Count to pic	289.00	92.00	942.00	108.00	63.00	952.00

Table VI. Some classical AE parameters of the six hits computed from the signal denoised by wavelet shrinkage in the case of an electric noise.

	hit_1	hit_2	hit_3	hit_4	hit_5	hit_6
Envelopes correlation	0.89	1.00	0.99	0.99	0.73	1.00
Kullback-Leiber distance	14.20	0.17	6.32	0.03	11.16	1.47
Absolute energy (MV)	122.04	1538.93	166.45	4136.92	141.59	270.79
Amplitude (V)	12.62	23.85	13.99	19.84	13.04	22.46
Count	1571.00	971.00	1515.00	250.00	309.00	4455.00
Mean frequency (kHz)	60.42	53.91	56.07	147.93	61.80	101.24
Rise Time (ms)	4.43	1.20	17.43	0.34	1.22	5.82
Count to pic	242.00	64.00	976.00	58.00	69.00	439.00

of the decomposition. The reader is referred to [23] for a more comprehensive description of the method.

Decomposition stage The first step of the decomposition is embedding. It consists in transforming the one-dimensional signal x into the multidimensional signal $(X_1, \ldots, X_K)$, where $X_i = (x_i, \ldots, x_{i+L-1})^T \in \mathbb{R}^L$ and $K = N - L + 1$. The vectors, called L-lagged vectors, are grouped into the trajectory matrix

$$\mathbf{X} = \left[X_1, \ldots, X_K\right] = (x_{ij})_{i,j=1}^{L,K}.$$

In the second step of the decomposition stage, a singular value decomposition (SVD) of the trajectory matrix is performed. Denote by $\lambda_1, \ldots, \lambda_L$ the eigenvalues of the matrix $\mathbf{XX^T}$ sorted in decreasing order of magnitude $(\lambda_1 \geq \lambda_2 \geq \ldots \lambda_L \geq 0)$, and by $U_1, \ldots, U_L$ the orthonormal system of the associated eigenvectors. Let $d = max\{i \; such \; that \; \lambda_i > 0\}$. If we consider $V_i = \mathbf{X}^T U_i / \sqrt{\lambda_i}$, the SVD of the trajectory matrix $\mathbf{X}$ can be then represented as a sum of rank-one bi-orthogonal elementary matrices $\mathbf{X}_i = \sqrt{\lambda_i} U_i V_i^T$ such that

$$\mathbf{X} = \mathbf{X}_1 + \cdots + \mathbf{X}_d.$$

The collection (λ_i, U_i, V_i) is called the ith eigentriple of the SVD.

Reconstruction Stage The reconstruction stage consists in partitioning the set of indices $\{1, \ldots, d\}$ into several groups, and then in summing the matrices within each group. Considering the group $I = \{i_1, \ldots, i_p\}$ and the associated matrix $\mathbf{X}_I$ defined as $\mathbf{X}_I = \mathbf{X}_{i_1}, \ldots, \mathbf{X}_{i_p}$, splitting the set of indices $\{I_1, \ldots, I_m\}$ leads to the decomposition

$$\mathbf{X} = \mathbf{X}_{I_1} + \cdots + \mathbf{X}_{Im}.$$

The procedure for choosing the set $\{I_1, \ldots, I_m\}$ is called the eigentriple grouping. Finally, the last step of SSA transforms each matrix resulting from the grouping stage into a new signal $\tilde{x}^{(k)}$ of the same length N as the initial

Author's complimentary copy

Table VII. Some classical AE parameters of the six hits computed from the signal denoised by the SSA in the case of an electric noise.

	hit_1	hit_2	hit_3	hit_4	hit_5	hit_6
Envelopes correlation	0.94	1.00	0.99	0.73	0.94	0.99
Kullback-Leiber distance	5.52	1.13	1.33	3.27	3.89	3.78
Absolute energy (MV)	12.23	1004.00	57.65	285.99	36.46	67.12
Amplitude (V)	3.70	20.78	10.23	10.95	6.76	16.93
Count	2936.00	1618.00	2716.00	222.00	581.00	5235.00
Mean frequency (kHz)	112.92	89.84	100.53	131.36	116.20	118.97
Rise Time (ms)	8.58	1.20	18.31	0.26	1.27	6.04
Count to pic	969.00	121.00	1807.00	34.00	146.00	707.00

Table VIII. Some classical AE parameters of the six hits computed from the signal denoised by the SS in the case of a mixed noise.

	hit_1	hit_2	hit_3	hit_4	hit_5	hit_6
Envelopes correlation	0.92	1.00	0.98	0.84	0.96	0.98
Kullback-Leiber distance	2.19	0.35	0.95	1.17	0.33	0.82
Absolute energy (MV)	0.70	886.31	14.32	1471.88	15.86	55.40
Amplitude (V)	-7.23	21.97	5.53	18.34	6.97	19.76
Count	2542.00	1199.00	2188.00	244.00	428.00	5131.00
Mean frequency (kHz)	97.77	66.57	80.98	144.38	85.60	116.61
Rise Time (ms)	6.42	1.20	18.31	0.30	1.27	6.04
Count to pic	525.00	141.00	1506.00	45.00	105.00	685.00

Table IX. Some classical AE parameters of the six hits computed from the signal denoised by wavelet shrinkage in the case of a mixed noise.

	hit_1	hit_2	hit_3	hit_4	hit_5	hit_6
Envelopes correlation	0.04	0.98	0.69	0.99	0.80	0.92
Kullback-Leiber distance	25.93	0.23	14.68	0.16	8.29	1.46
Absolute energy (MV)	4.24	613.75	6.80	1979.55	9.07	50.51
Amplitude (V)	-7.75	22.47	5.37	18.29	5.98	19.63
Count	85.00	396.00	244.00	232.00	16.00	283.00
Mean frequency (kHz)	3.27	21.99	9.03	137.28	3.20	6.43
Rise Time (ms)	6.51	1.20	18.31	0.34	1.27	6.04
Count to pic	37.00	11.00	180.00	54.00	5.00	56.00

signal x such that

$$x_t = \sum_{k=1}^{m} \tilde{x}_t^{(k)}.$$

Note that two crucial parameters have to be taken into account in SSA implementation. The choice of the window length L ($2 \leq L \leq N$) determines the quality of the decomposition, and the separability between the reconstructed signals allows to evaluate the effectiveness of the processing. In the case of AE signal denoising for example, a good separation of the estimated source signal $\hat{s}$ from the estimated noise $\hat{n}$ is expected.

2.2.1. Detection of structural changes by SSA

The detection of structural changes is based on the assumption that pure noise segments of the received signal x are governed by a linear recurrent formulae (LRF) (see [23], chap.3 and 5). The violations of this property correspond to structural changes and then to segments associated to a potential source mechanism. From a practical point of view, the structural changes are detected by using the heterogeneity matrix (H-matrix). The rows of this matrix can be described as the homogeneity of x relatively to a fixed segment (see [23], chap.3 and 5).

2.2.2. SSA denoising

According to the type of noise, different denoising strategies have been proposed in [24]. In the case of a noise with a narrowband spectrum, a direct SSA applied with the correct grouping strategy of the eigenvectors leads to excellent results. For a more complex noise, a two-step denoising method has been proposed. In the first step, a function for the detection of structural changes is created by using the H-matrix. This function is then applied to the corrupted signal in order to get a pre-processed signal. The second step consists in applying a SSA of the pre-processed signal in order to obtain the final estimator of the source signal.

2.3. Wavelet transforms

Development of wavelet transforms over the last two decades has revolutionized modern signal and image pro-

Author's complimentary copy

Table X. Some classical AE parameters of the six hits computed from the signal denoised by SSA in the case of a mixed noise.

	hit_1	hit_2	hit_3	hit_4	hit_5	hit_6
Envelopes correlation	0.95	0.99	0.98	0.83	0.93	0.97
Kullback-Leiber distance	3.70	1.62	1.40	2.76	2.48	4.95
Absolute energy (MV)	12.75	915.26	56.67	572.11	38.11	68.01
Amplitude (V)	2.96	20.06	9.14	14.44	7.72	16.48
Count	2886.00	1638.00	2749.00	246.00	568.00	5287.00
Mean frequency (kHz)	111.00	90.95	101.75	145.56	113.60	120.15
Rise Time (ms)	4.76	1.22	18.31	0.26	1.27	6.19
Count to pic	537.00	115.00	1837.00	37.00	139.00	748.00

Table XI. Some classical AE parameters of the six hits computed from the signal denoised by SS in the case of the sum of all types of noise.

	hit_1	hit_2	hit_3	hit_4	hit_5	hit_6
Envelopes correlation	0.68	1.00	0.95	0.58	0.89	0.97
Kullback-Leiber distance	6.91	0.41	1.26	1.06	2.69	0.87
Absolute energy (MV)	1.25	756.56	13.39	717.59	3.41	41.96
Amplitude (V)	-8.67	22.08	4.17	12.68	-3.69	18.96
Count	3305.00	1617.00	2958.00	254.00	606.00	5567.00
Mean frequency (kHz)	127.12	89.78	109.48	150.30	121.20	126.52
Rise Time (ms)	4.89	1.20	18.31	0.72	1.27	6.04
Count to pic	629.00	128.00	1987.00	115.00	125.00	816.00

cessing, especially in the field of signal denoising [13]. Wavelet transforms are used for both detection of structural changes and denoising.

2.3.1. Detection of structural changes by wavelet transform

A wavelet transform of x is a multiresolution decomposition of x which allows to display and analyze the characteristics of x dependent on time and scale. Given a mother wavelet $\psi(t)$, the continuous wavelet transform (CWT) of the signal x is a two-variable function defined by

$$CWT(a,b) = \frac{1}{\sqrt{a}} \int_{-\infty}^{\infty} \psi\left(\frac{t-b}{a}\right) x(t)\,\mathrm{d}t,$$

where a is the scale or dilation parameter corresponding to the frequency, and b the translation parameter related to the location of the wavelet function. $CWT(a,b)$ is the correlation between the signal $x(t)$ and the son wavelet $\psi_{a,b}(t)$. The discrete wavelet transform (DWT) is a sampled version of the CWT computed by replacing $a, b \in \mathbb{R}$ by a discrete grid

$$a = 2^{-j}, \quad b = k2^{-j}, \quad j,k \in \mathbb{Z}.$$

For more details on the computational aspects of the CWT and the DWT, the reader can refer to [25, 26, 27]. In practice, the key points to take into account when using a wavelet transform are the choice of the mother wavelet and the scale parameter (or resolution level). The mother wavelet should be chosen such that it is able to well characterize the signal. This can be decided according to the correlation between the wavelet and the signal. The choice of the resolution level depends on the complexity of the analyzed signal. When the structure of the signal x becomes more and more complex, one needs to use increasing order levels in order to isolate its fine details.

2.3.2. Wavelet denoising

Most of wavelet-denoising methods proposed in the literature are based on a thresholding approach which uses the orthogonality property of the son wavelets in order to decompose the received signal at the level j and the index k as (see [13])

$$x_{jk} = s_{jk} + n_{jk},$$

where the noise n is supposed to be random. As the coefficients of wavelets are usually sparse for the source signal s, the denoising problem associated with Eq.(2) reduces to recovering the coefficients of s which are relatively stronger than those related to the random noise n (see [13] and [27],chap.10). This is done by thresholding (i.e. by defining a function which makes it possible to decide whether or not a given coefficient is associated with the noise).

In practice, two important points, however not enough addressed in the literature, are the choice of the mother wavelet and the choice of the desired number of resolution level. The wavelet should be chosen according to the same process as for the case of the detection of structural changes presented above. The choice of the number of the decomposition level is trickier, since it depends on several factors among which the most important is the noise behavior. In the case of noticeable noise, for example, one may need increasing order levels in order to get the fine details of the signal [13].

Author's complimentary copy

Table XII. Some classical AE parameters of the six hits computed from the signal denoised by wavelet shrinkage in the case of the sum of all types of noise.

	hit_1	hit_2	hit_3	hit_4	hit_5	hit_6
Envelopes correlation	0.44	0.99	0.89	0.99	0.86	0.94
Kullback-Leiber distance	14.39	0.13	2.78	0.12	1.96	0.49
Absolute energy (MV)	1.42	645.63	4.15	1961.79	6.93	50.05
Amplitude (V)	-2.69	22.71	4.89	18.22	5.45	20.32
Count	511.00	603.00	726.00	240.00	110.00	934.00
Mean frequency (kHz)	19.65	33.48	26.87	142.01	22.00	21.23
Rise Time (ms)	12.97	1.20	18.31	0.34	1.27	6.04
Count to pic	292.00	31.00	492.00	56.00	34.00	145.00

Table XIII. Some classical AE parameters of the six hits computed from the signal denoised by SSA in the case of the sum of all types of noise.

	hit_1	hit_2	hit_3	hit_4	hit_5	hit_6
Envelopes correlation	0.94	0.99	0.96	0.75	0.92	0.89
Kullback-Leiber distance	8.72	1.63	2.99	1.95	6.27	4.85
Absolute energy (MV)	18.24	1025.53	68.00	820.34	51.70	53.53
Amplitude (V)	3.37	20.48	9.54	13.35	7.16	17.01
Count	3418.00	1941.00	3371.00	262.00	681.00	5493.00
Mean frequency (kHz)	131.46	107.77	124.77	155.03	136.20	124.83
Rise Time (ms)	6.78	1.20	16.62	0.22	1.27	6.04
Count to pic	928.00	116.00	2070.00	39.00	164.00	826.00

3. Detection of structural changes

Two types of SNR context must be considered here.

In a high SNR context, a simple thresholding (i.e. using a threshold equal or slightly above the level of the noise) would be sufficient to detect the structural changes associated with the hits having a significant energy. However, as depicted in Figure 7a, detecting by thresholding the low energetic hits is quite challenging. In order to get detailed information about the different hits and to analyze the relationships between them, some of the methods presented in Section 2 are then advisable. In a high SNR context (e.g. 10 dB of SNR), all the methods proposed for the detection of structural changes allow to detect the six hits, regardless the type of noise (Figure 7). However, for a finer analysis of the structure of x, the CWT is a better tool than the STFT. The SSA can be used as a complementary tool to the CWT. Indeed, according to the chosen strategy of construction of the H-matrix, one can explore if the different segments of x exhibit a chosen information and at which level they are correlated according to this information (see [24]).

In a very low SNR context (e.g. -10 dB of SNR), the thresholding becomes totally inefficient. Then, sophisticated methods such as those presented in Section 2 become necessary in order to cope with the detection problem. However, the detectability of the hits depends on the type of noise. The most challenging situation corresponds to noises with a very wide-band spectrum (e.g. gaussian noises). In these cases, the H-matrix has the best potential for hit detection (Figure 8). This is mainly due to the flexibility of the SSA for selecting the linear spaces which span the base subsignals (see [24]). When the noise has its energy concentrated in a specific frequency band (e.g. electric noise or mixed noise), the best method for the structural analysis remains the CWT.

4. Denoising

When the SNR is low enough that the detection of structural changes may be a difficult task, or when the experimentalists are interested in the identification of the physical phenomena associated with AE events, it becomes necessary to first denoise the AE signals in order to get more effectiveness in the result interpretation. Barat et al [12] have proposed different signal processing methods which can be applied more or less successfully according to the type of noise. Here, we test the different methods presented in Section 2 for denoising signals corrupted by the different types of noise of interest (Figure 5). These methods are applied alone or jointly in order to improve their performances.

4.1. Comparative study of the selected methods

Considering the SNR improvement ratios reported in Table XIV, the qualitative evaluation based on the whole experimental signal shows that the SS and the SSA methods are robust to changes in the stochastic behavior of noise. However, the SS has higher SNR improvement ratios. This can be easily explained theoretically. Indeed, the SS method uses the physical hypothesis of the availability of an estimator $\hat{n}$ of the noise n, whereas the wavelet shrinkage method needs a random noise and the SSA method a

Author's complimentary copy

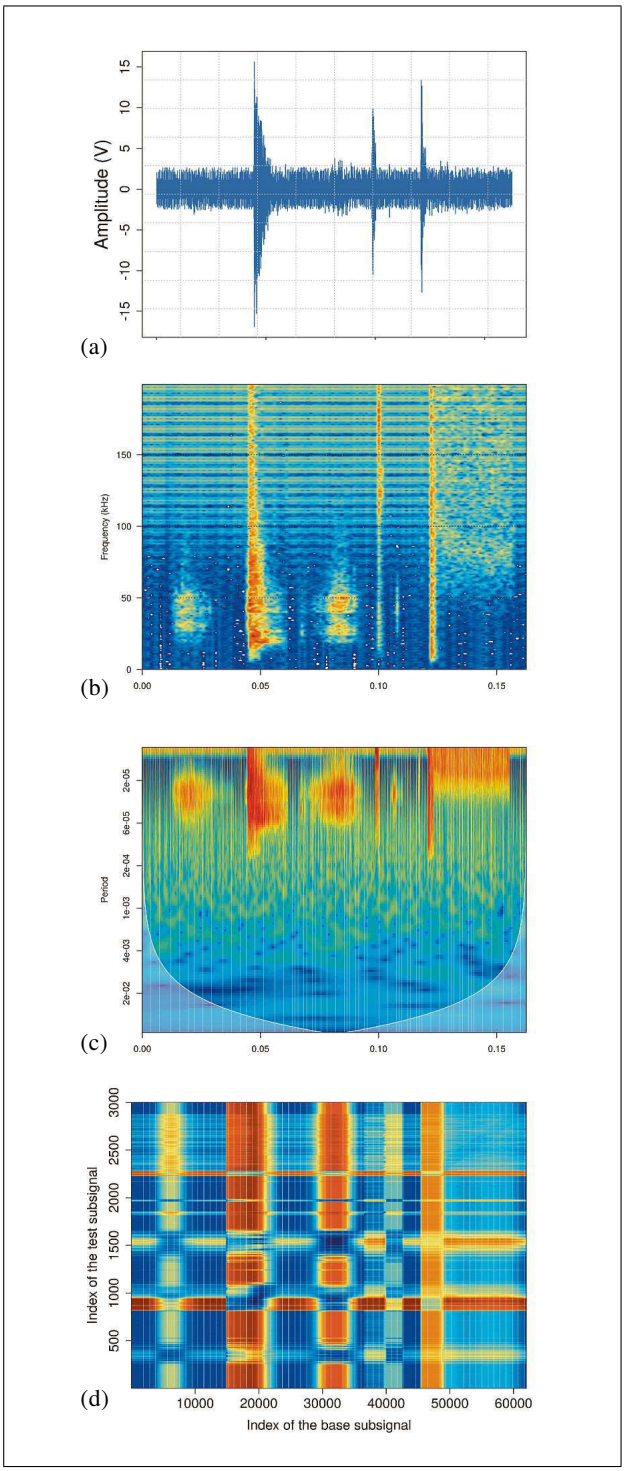

Figure 7. Detection of the structural changes in high SNR context (10 dB), in the case of the source signal corrupted by an electric noise (a), by using the STFT with a hanning window of length $\beta = 512$ (b), the CWT with a morlet wavelet (c), and the H-matrix with $B = 300$, $T = 3000$, $L = 100$ and $\mathcal{L}_r^{(1)} = span(U_1^1, \ldots, U_1^{30})$ (d). See [24] for details about the H-matrix parameters.

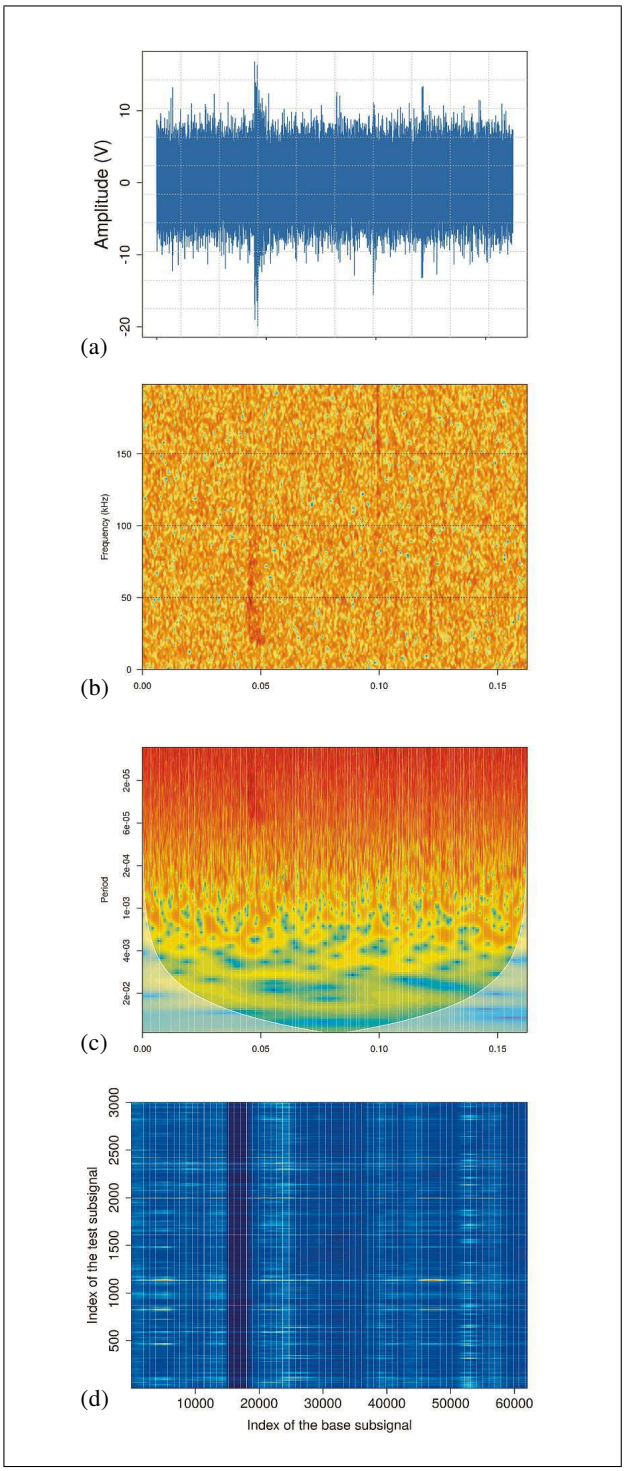

Figure 8. Detection of the structural changes in low SNR context (-10 dB), in the case of the noise-free experimental signal corrupted by a gaussian white noise (a), by using the STFT with a hanning window of length $\beta = 256$ (b), the CWT with a morlet wavelet (c), and the H-matrix with $B = 300$, $T = 3000$, $L = 100$ $\mathcal{L}_r^{(1)} = span\{U_i^1, max(|FT(U_i^1)|) \in [40, 60]\ kHz\}$ (d). See [24] for details about the H-matrix parameters.

good separability between the source signal and the noise. Therefore, if $\hat{n}$ correctly estimates n, as it is the case here, the SS method provides the most robust results. However, we also observe that the SS method always presents some residual noises, whatever the type of noise (Figure 10a).

It is well known that the wavelet shrinkage method gives excellent results in the case of a gaussian white noise.

Author's complimentary copy

Table XIV. SNR improvement ratios as a function of the type of noise and the denoising method. Global SNR for x is 5 dB. Ratios are calculated using: ratio = $(\mathrm{SNR}_{\mathrm{output}} - \mathrm{SNR}_{\mathrm{input}}/(\mathrm{SNR}_{\mathrm{input}})$. W.s.: Wavelets shrinkage.

	SS	W.s.	SSA
Gaussian noise	3.52	9.31	3.42
Electric noise	5.73	1.62	4.00
Mixed noise	6.68	3.42	3.50
Sum of all the types noises	4.63	4.49	3.36

Therefore, it should be preferred to other methods in this case. However, when some noise components are deterministic (e.g. electric noise, mixed noise...), the wavelet shrinkage method can be fully inefficient (Fig 9) or keeps some strong noise residuals (Figure 10b). As a consequence, an additional method should be combined with the wavelet shrinkage method in order to efficiently preprocess the signal s.

The results of the SSA method are globally slightly worse than those of the SS and wavelet shrinkage methods. However, as concluded in [24], the SSA method has a great interest since it becomes an excellent denoising method once the separability problem solved. A new strategy to do this is proposed in the following.

4.2. Impact of the selected methods on the AE parameters

For an effective interpretation of the denoised signals, it is of major interest to have an a priori knowledge about the potential bias, introduced by a selected method, on the identification of the source mechanisms. We then compare some classically used AE parameters computed from the noise-free events (Figure 3 and Table I) with those computed from the signals denoised using the different selected methods, and for the different types of noise under consideration in this paper (Tables II–XIII). We note that whatever the type of noise and the denoising method used, the AE parameters associated with the waveform are better restored than those associated with the acoustic activity and the frequency content. Indeed, the envelope, the rise time, and the amplitude of the hits associated with the denoised signals are close to those of the noise-free hits in all cases. On the contrary, the estimations of the count, of the mean frequency, and of the count-to-peak exhibit significant bias in comparison with those of the noise-free hits. However, the latter result must be moderated by the fact that the global shape of the spectra of the signals associated with the source mechanisms of interest is well restored in the case of optimal use conditions for the denoising method (e.g. the wavelet shrinkage method in the case of a gaussian white noise, or the SS method in the case of an electric noise), since the Kullback-Leiber distances are small. Furthermore, the results also show that, except for the case of the electric noise for which the result of the wavelet shrinkage method is obviously inefficient, there is no clear hierarchy between the different methods

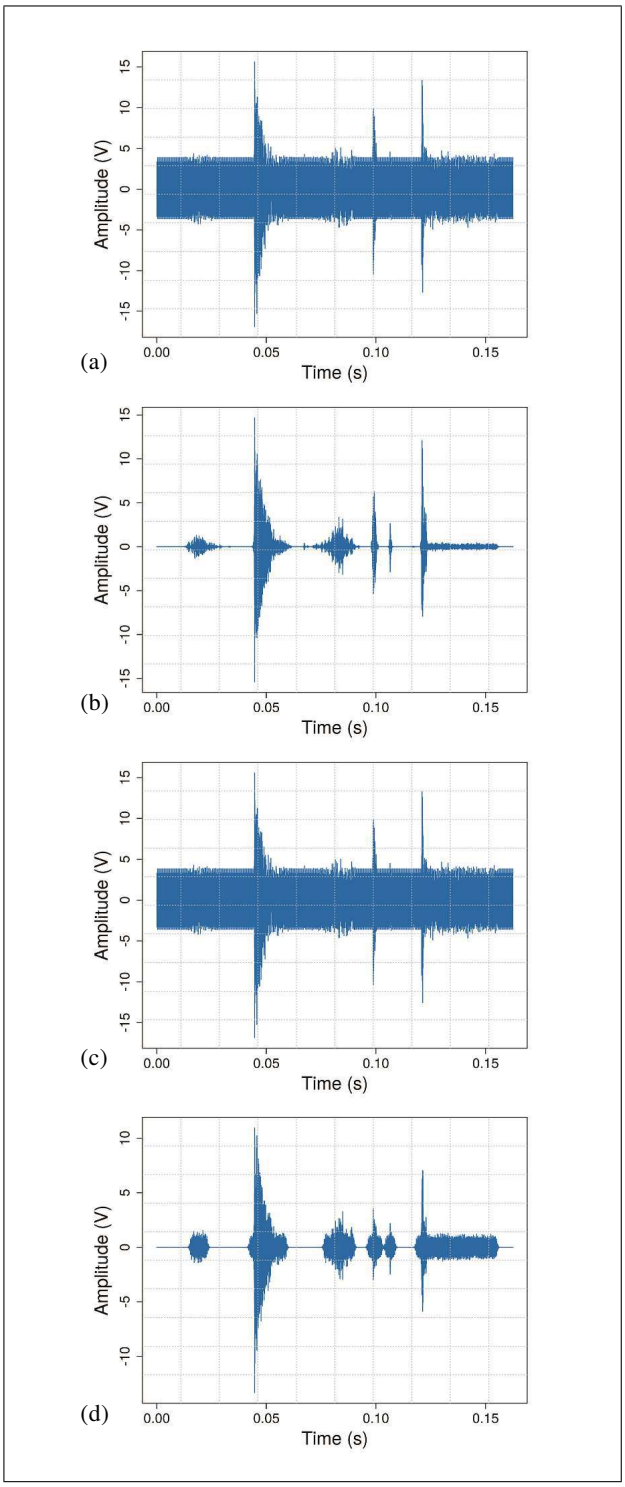

Figure 9. Signal denoising result (estimation of s) in the case of an electric noise with an initial SNR of 5 dB. (a) noisy signal x, (b) SS denoising result with an overlapping window length of 512 and an over-subtraction parameter $\alpha = 4$, (c) wavelet shrinkage result with a soft thresholding with a sureShrink function, (d) two-step SSA denoising result with $B = 300$, $T = 2000$, $L = 100$ and $\mathcal{L}_r^{(1)} = span(U_1^1, \ldots, U_1^{10})$ in the first step; and $L = 500$ in the second step See [24] for details about the H-matrix parameters.

Author's complimentary copy

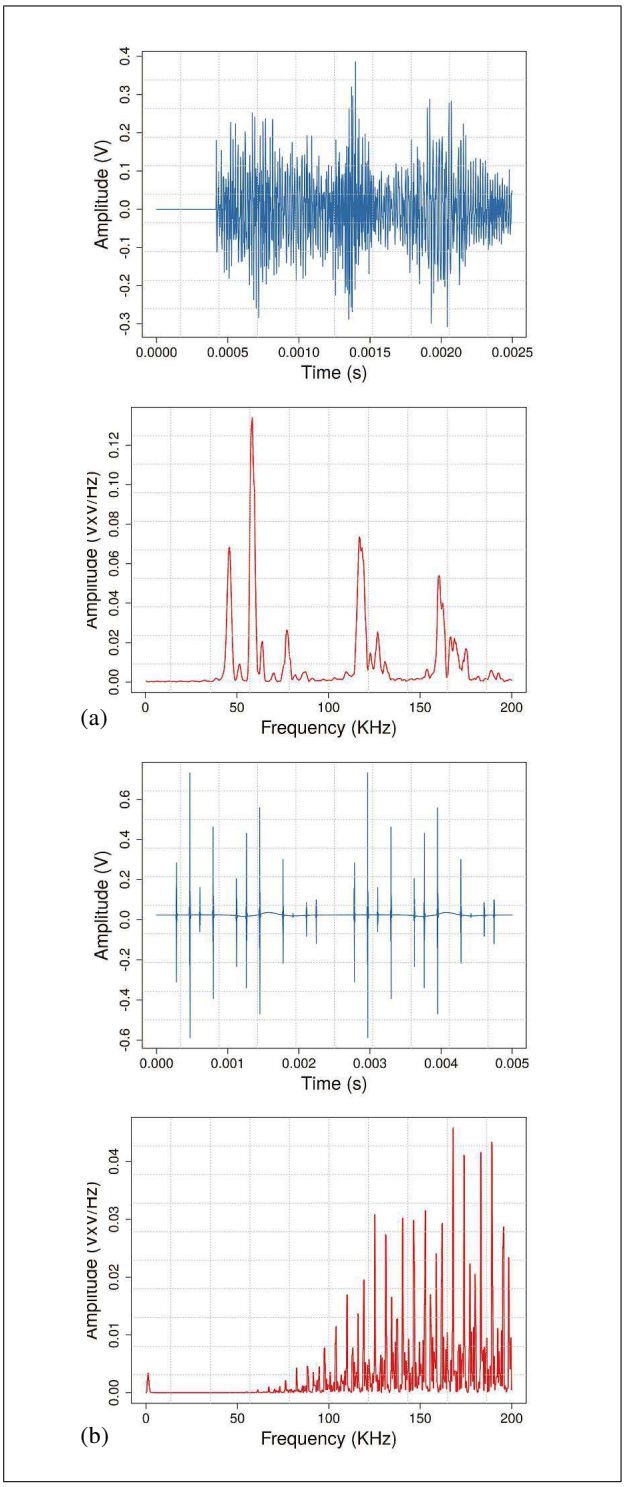

Figure 10. Residual noises resulting from the application of the SS method for a gaussian white noise context (a), and from the application of the wavelet shrinkage method for the case of the sum of all types of noises (b).

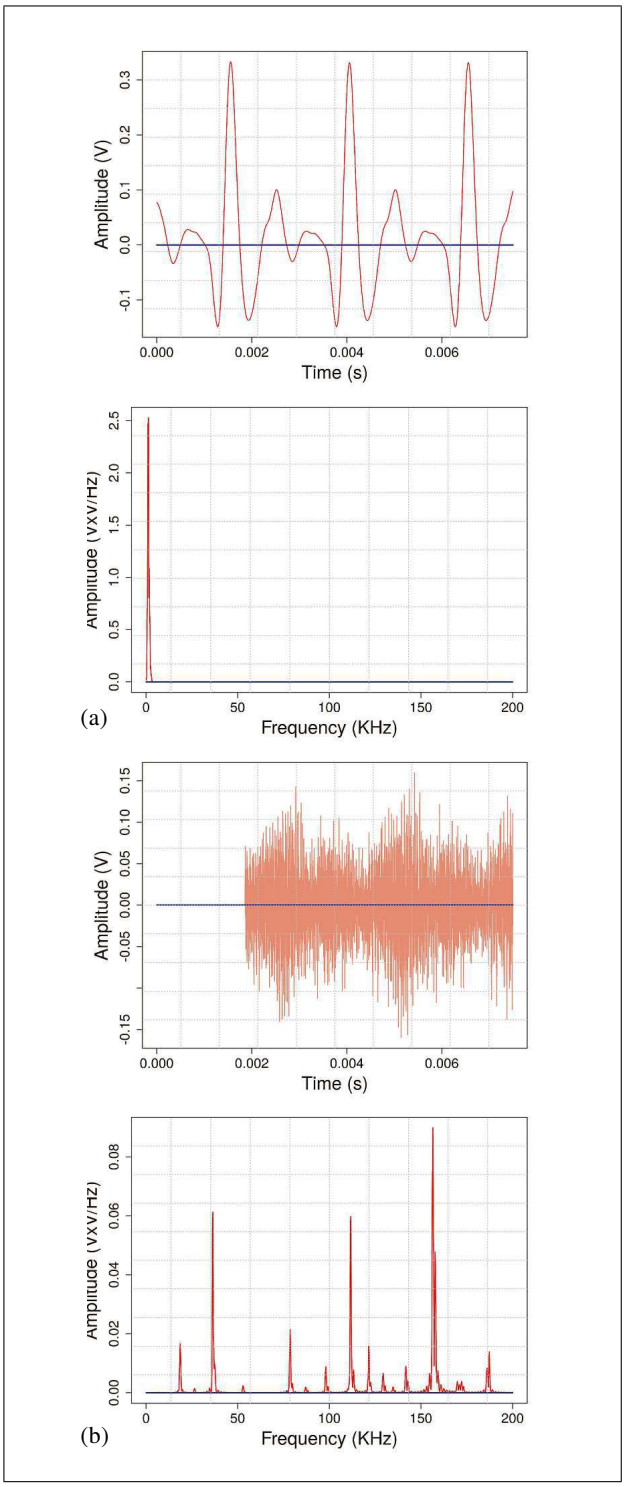

Figure 11. Illustration of the removing of the residual noise by combining (a) the frequency-selective filtering and the wavelet shrinkage in mixed noise context and (b) the SS and the wavelet shrinkage in the case of the sum of all types of noise. The residual noise is indicated in red and the improvement result in blue.

in terms of ability to restore the noise-free signal waveform and frequency characteristics. As a consequence, the SNR improvement ratio remains the most efficient criterion when choosing a denoising method.

4.3. Combining different methods to improve denoising

When the residual noise or its spectrum clearly highlights a lack of efficiency of the selected denoising method to remove some deterministic noise components (Figure 10), it is necessary to go ahead with the noise processing. Com-

Author's complimentary copy

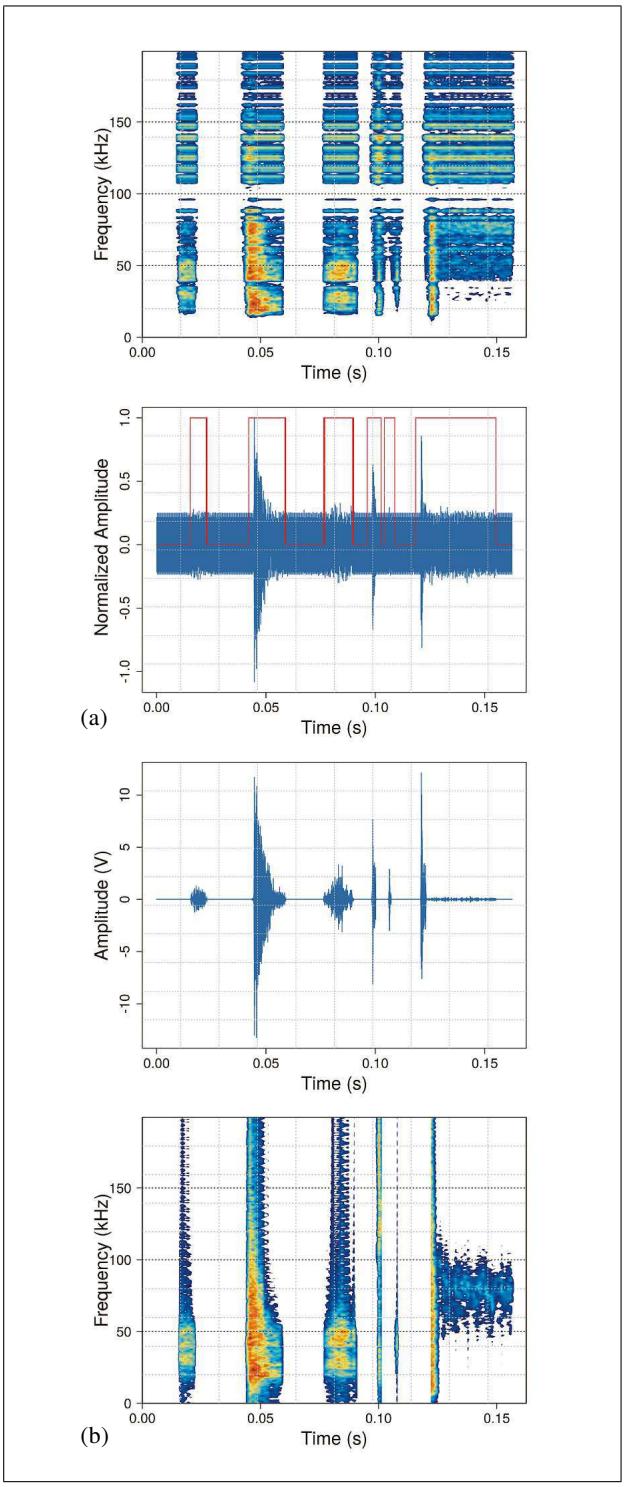

Figure 12. Illustration of the SSA improvement by combination with the SS method : (a) spectrogram of the result of the two-step SSA denoising, (b) superposition of the function of detection of structural changes and the noisy signal, (c) denoised signal (to be compared with Figure 9d) and (d) spectrogram of the denoised signal.

bining the selected method with other ones is then an efficient procedure to get excellent denoising results.

Let us first consider the wavelet shrinkage method. When the residual noise spectrum is mainly narrow-band, several approaches can be used in order to reduce its impact, the simplest one being to use a frequency selective filter [28, 29] in order to remove the deterministic component prior to the wavelet shrinkage (Figure 11a). A DWT and a SSA decomposition can also be used in order to get the same results. For a residual noise with a wide-band spectrum (e.g., an electric noise), using a SS prior to the wavelet shrinkage leads to excellent results.

Let us now consider the SS method. If $\hat{n}$ correctly estimates n, the residual noise can always be removed by increasing the over-subtraction parameter α. Unfortunately, this leads to considerably reduce the energy of the restored signal, and sometimes to corrupt its waveform. For a more effective removal of the residual noise, it is thus better to use a wavelet shrinkage after the SS (Figure 11b).

The main limitation of the SSA denoising lies in the introduction of artifacts when the separability between the source signal s and the noise n is lacking (generally, in wide-band noise contexts). In order to cope with this fundamental limitation, we propose to combine the two-step strategy proposed in [24] with the SS method. We keep the first step of this denoising strategy, which is based on the H-matrix and consists in the detection and the removing of the pure noise segments of the signal. The second step, consisting in a SSA decomposition of the pre-processed signal resulting from the first step, is then replaced by a SS. Figure 12 shows that this approach leads to a significant improvement of denoising.

5. Conclusion

AE signals recorded from nuclear safety experiments are contaminated by different kinds of noise whose level can be significant compared to signal. Therefore, prior to identification of the source mechanisms associated with the acoustic events of interest, the noisy AE signals must be properly denoised.

In this paper, we have evaluated the ability and efficiency of several methods for detecting structural changes and denoising AE signals, according to the stochastic behavior of the noise and its level. One conclusion of this work is that there is no absolute method which is efficient regardless the type of noise and its level. The limitations of a simple thresholding for detecting structural changes have been highlighted, even in high SNR context. We have shown that the continuous wavelet transform method is the best tool for analysis of the signal structure in high SNR context, whatever the type of noise. On the contrary, in low SNR context, the detectability of the AE events strongly depends on the type of noise. For the case of a wide-band noise, the detection becomes a challenging task and only the singular spectrum analysis method allows to detect some hits, generally the most energetic ones.

The denoising problem has been considered from several points of view. If we consider only the global SNR improvement ratio, the spectral subtraction method is the most robust to changes in the stochastic behavior of noise. However, in some specific cases, it is preferable to use other methods like the frequency selective filtering, the

Author's complimentary copy

wavelet shrinkage method or the singular spectrum analysis method. In order to further improve the denoising efficiency and to get excellent results regardless the type of noise and its level, we have suggested to combine different methods. Finally, the analysis of the impact of the different selected denoising methods on some classically used AE parameters shows that, whatever the type of noise and the denoising method, AE parameters associated with the waveform are better restored than those associated with the acoustic activity and the frequency content.

Acknowledgement

The authors thank the reviewers for constructive and relevant suggestions which have improved the paper and will be useful for our future works.

References

[1] Q. Ai, C. Liu, X. Chen, P. He, Y. Wang: Acoustic emission of fatigue crack in pressure pipe under cyclic pressure. Nuclear Engineering and Design. **240** (2010) 3616–3620.

[2] D. S. Kupperman, T. N. Claytor, R. Groenwald: Acoustic leak detection for reactor coolant systems. Nuclear Engineering and Design **86** (1985) 13–20.

[3] C. B. Scruby, H. N. Wadley: An assessment of acoustic emission for nuclear pressure vessel monitoring. Progress in Nuclear Energy **11** (1983) 275–297.

[4] S. P. Ying: The use of acoustic emission for assessing the integrity of a nuclear reactor pressure vessel. NDT International **12** (1979) 175–179.

[5] A. Sinclair, D. C. Connors, C. L. Formby: Acoustic emission analysis during fatigue crack growth in steel. Materials Science and Engineering **28** (1977) 263–273.

[6] L. Hégron, P. Sornay, N. Favretto-Cristini: Compaction of a bed of fragmentable particles and associated acoustic emission. IEEE Transactions on Nuclear Science **61** (2014) 2175–2181.

[7] N. Favretto-Cristini, L. Hégron, P. Sornay: Identification of the fragmentation of brittle particles during compaction process by the acoustic emission technique. Ultrasonics **67** (2016) 178–189.

[8] J. Roget: Essais non destructifs: L'émission acoustique: Mise en œuvre et applications. AFNOR; CETIM, 1988.

[9] G. Gautschi: Piezoelectric sensorics: force, strain, pressure, acceleration and acoustic emission sensors, materials and amplifiers. Springer Science & Business Media, 2002.

[10] C. U. Grosse, M. Ohtsu: Acoustic emission testing. Springer Science & Business Media, 2008.

[11] S. Sriram, S. Nitin, K. M. M. Prabhu, M. J. Bastiaans: Signal denoising techniques for partial discharge measurements. IEEE Transactions on Dielectrics and Electrical Insulation **12** (2005) 1182–1191.

[12] V. Barat, Y. Borodin, A. Kuzmin: Intelligent acoustic emission signal filtering methods. Journal of Acoustic Emission **28** (2010) 109–119.

[13] R. Cohen: Signal denoising using wavelets. Project Report, Department of Electrical Engineering Technion, Israel Institute of Technology, Haifa (2012).

[14] M. Kharrat, E. Ramasso, V. Placet, M. L. Boubakar: A signal processing approach for enhanced acoustic emission data analysis in high activity systems: application to organic matrix composites. Mechanical Systems and Signal Processing **70** (2016) 1038–1055.

[15] L. O. Jernkvist, A. R. Massih: Nuclear fuel behavior under reactivity-initiated accident (ria) conditions. Tech. Rept. Nuclear Energy Agency, 2010.

[16] L. Pantera, O. I. Traore: Reproducible data processing research for the CABRI RIA experiments acoustic emission signal analysis. Advancements in Nuclear Instrumentation Measurement Methods and their Applications (ANIMMA), 2015 4th International Conference on, 2015, IEEE, 1–8.

[17] S. F. Boll: Suppression of acoustic noise in speech using spectral subtraction. IEEE Transactions on Acoustics, Speech and Signal Processing **27** (1979) 113–120.

[18] M. Berouti, R. Schwartz, J. Makhoul: Enhancement of speech corrupted by acoustic noise. Acoustics, Speech, and Signal Processing, IEEE International Conference on ICASSP'79., 1979, IEEE, 208–211.

[19] A. Chokkarapu, S. C. Uppalapati, A. Chintakuntla: Implementation of spectral subtraction noise suppressor using DSP processor. International Journal of Computer Science and Telecommunications **4** (2013) 29–33.

[20] T. Matsuo, H. Cho: Development of AE monitoring system with noise reduction function by spectral subtraction. Materials Transactions **53** (2012) 342–348.

[21] O. I. Traoré, L. Pantera, N. Favretto-Cristini, S. Viguier-Pla: Emission acoustique et traitement du bruit : cas de signaux expérimentaux en contexte nucléaire. 13e Congrès Français d'Acoustique, Le Mans, France, Apr. 2016.

[22] S. V. Vaseghi: Advanced digital signal processing and noise reduction. John Wiley & Sons, 2008.

[23] N. Golyandina, V. Nekrutkin, A. A. Zhigljavsky: Analysis of time series structure: SSA and related techniques. CRC Press, 2001.

[24] O. I. Traore, L. Pantera, N. Favretto-Cristini, P. Cristini, S. Viguier-Pla, P. Vieu: Structure analysis and denoising using singular spectrum analysis: application to acoustic emission signals from nuclear safety experiments. Measurement **104** (2017) 78 – 88.

[25] J. Sadowsky: Investigation of signal characteristics using the continuous wavelet transform. Johns Hopkins APL technical digest **17** (1996) 258–269.

[26] S. Mallat: A wavelet tour of signal processing. Academic Press, 1999.

[27] D. B. Percival, A. T. Walden: Wavelet methods for time series analysis. Vol. 4. Cambridge University Press, 2006.

[28] T. W. Parks, C. S. Burrus: Digital filter design. Wiley-Interscience, 1987.

[29] J. G. ProaKis, D. G. Manolakis: Digital signal processing: Principles, algorithms and applications. 4 ed. Pearson Prentice Hall, 2007.

Author's complimentary copy